Polymer 50 (2009) 3587–3594

Contents lists available at ScienceDirect

Polymer

journal homepage: www.elsevier.com/locate/polymer

Synthesis, characterization and UV curing kinetics of hyperbranched polysiloxysilanes from A_2 and CB_2 type monomers

Sheng-Jie Wang [a,b,*], Xiao-Dong Fan [b], Jie Kong [b,**], Jian-Ren Lu [c]

[a] Center for Bioengineering and Biotechnology, China University of Petroleum, Qingdao 266555, PR China
[b] Department of Applied Chemistry, School of Science, Northwestern Polytechnical University, Xi'an 710072, PR China
[c] Biological Physics Group, School of Physics and Astronomy, University of Manchester, Schuster Building, Manchester M139JP, UK

ARTICLE INFO

Article history:
Received 28 December 2008
Received in revised form
5 May 2009
Accepted 25 May 2009
Available online 2 June 2009

Keywords:
Hyperbranched polysiloxysilanes
A_2 and CB_2 type monomers
UV curing kinetics

ABSTRACT

A controllable approach to synthesize UV curable hyperbranched polysiloxysilanes from A_2 (1,1,3,3-tetramethyldisiloxane) and CB_2 type monomers (methyl(vinyl)silanediylbis(oxy)bis(ethane-2,1-diyl) diacrylate and methyl(vinyl) silanediylbis(oxy)bis(ethane-2,1-diyl)bis(2-methylacrylate)) was developed in the presented paper. The polymerization was monitored using FTIR, where a two-step polyaddition mode was observed. Vinyl silane group preferentially reacted with hydride silane, resulting in the formation of AB_2 type intermediates containing one hydride silane and two acrylate (or methacrylate) groups, at the same time, there may be low quantity of B_4 type intermediates. The intermediates further polymerized to form hyperbranched polymers. The UV curing kinetics of the hyperbranched polymers, especially the effects of atmosphere, content of photoinitiator and light intensity on UV curing behavior were studied in detail. The results indicated that the hyperbranched polymers could be cured rapidly under UV irradiation. The curing rates increased with the enhancement of light intensity, and the inhibition effect of oxygen could be restrained by increasing light intensity.

1. Introduction

Highly branched polymers, including dendrimers and hyperbranched polymers, have attracted a great deal of attention over the past two decades due to their unique physical and chemical properties as well as their potential applications in coatings, additives, catalysts, drugs and gene delivery, nanotechnology, and supramolecular science [1–6]. Dendrimers with perfect branched-structures and uniform molecular weights are usually synthesized by multi-step reactions with tedious isolation and purification procedures. In contrast, hyperbranched polymers, having similar properties with dendrimers and less perfect molecular structures, can be obtained via one-pot synthesis [7–9]. Recently, some effective synthesis approaches including couple monomer methodology and core dilution/slow addition method have been developed to control the molecular structure and molecular weight of hyperbranched polymers [1,10]. Therefore, hyperbranched polymers, such as polyphenylenes, polyesters, polyethers, polyurethanes, and organosilicon polymers, have become especially appealing in either laboratory or commercial preparations. Particularly, the investigation of siloxy-type hyperbranched organosilicon polymers with terminal silicon hydride or alkene groups is attractive due to their excellent thermal properties and feasibility in chemical modification [11].

Currently, organosilicon polymers including polysilazane, polycarbosilazane, polycarbosilane and polysiloxysilane are widely used as precursors for high performance ceramic materials [12–15]. Comparing with traditional linear organosilicon polymers, their hyperbranched homologues possess lower viscosity, excellent solubility and penetrability, and high reactivity. In addition, UV irradiation is extended and feasible to fabricate ceramic devices with complex structures and near shapes using less processing steps or free mould process [16–18]. Therefore, development of UV curable hyperbranched organosilicon polymers is attractive for realizing potential benefits of these polymers in high performance ceramic materials.

Hyperbranched organosilicon polymers with vinyl or allyl end groups have been prepared in our previous works [19–22]. However, even with large amounts of photoinitiator or at high temperature, the photo cross-linking speed of these polymers was lower than that of acrylates and methacrylates polymers [23–26].

* Corresponding author. Center for Bioengineering and Biotechnology, China University of Petroleum, Qingdao 266555, PR China. Tel.: +86 532 86981562.
** Corresponding author. Tel.: +86 29 88431688.
E-mail addresses: wang_shengjie@yahoo.com.cn (S.-J. Wang), mfkongjie@hotmail.com (J. Kong).

0032-3861/$ – see front matter © 2009 Elsevier Ltd. All rights reserved.
doi:10.1016/j.polymer.2009.05.049

Introducing active diluents in bulk UV curable polymers is an effective way to improve the UV curing speed, however, the system is inhomogeneous at the molecular level and the ceramic yields will be decreased with increasing the content of active diluents [22]. Therefore, the exploration of new hyperbranched organosilicon polymers, which could be cured more rapidly under UV irradiation, is one of urgent and important issues to improve feasibility on fabricating complex ceramic devices using less processing steps or free mould process.

In the presented paper, the hyperbranched polysiloxysilanes with high UV curing speed were prepared by employing "A_2 + CB_2 monomers" approach. The molecular structure, viscosity, molecular weight and the polydispersity of the resultant hyperbranched polymers were regulated by means of varying feeding ratio of two monomers. The UV curing kinetics of the hyperbranched polymers synthesized, especially the effects of atmosphere, content of photoinitiator, light intensity on UV curing behavior was studied in detail.

2. Experimental sections

2.1. Materials

Vinylmethyldichlorosilane (≥99%) was obtained from Center Research of New Silicone Materials of Wuhan University in China. 2-Hydroxyethyl acrylate (HEA) and 2-hydroxyethyl methacrylate (HEMA) were purchased from Xi'an Organic Chemical Reagents Corporation in China. Chloroplatinic acid (39%, platinum) was provided by Shannxi Kaida Chemical Ltd. in China. 4-Dimethylamino pyridine (DMAP) was obtained from Zhejiang Jintan Chemical Plant in China. Pyridine (AR), tetrahydrofuran (AR), hexane (AR), and other solvents were obtained from Tianjin Kermel Chemical Reagents Development Center in China. 2-Hydroxy-2-methyl-1-(4-*tert*-butyl) phenyl-propane-1-one (IHT-PI 185) was received from Insight High Technology Co. Ltd. in China. All solvents and silane monomers were distilled and dried with 4 Å grade molecular sieves before use.

2.2. Synthesis

2.2.1. Synthesis of M1

2-Hydroxyethyl acrylate (24.36 g, 0.21 mol), pyridine (16.6 g, 0.21 mol), 4-dimethylamino pyridine (0.1 g) and hexane (60 mL) were charged into a three-necked flask equipped with an addition funnel, a mechanical stirrer, a nitrogen inlet, and cooled in an ice bath. This system was mixed for 10 min at 0 °C in nitrogen atmosphere. A solution of vinylmethyldichlorosilane (13 mL, 0.10 mol) and hexane (25 mL) was added at a rate of 20 drops per minute. After stirring for 30 min at 0 °C, the system was heated to 15 °C and stirred for 6 h. After filtering the precipitated pyridine hydrochloride, the filtrate was washed with distilled water four times, and dried with anhydrous magnesium sulfate overnight. The solvent was removed via evaporation under reduced pressure. Then the desired monomer M1 (methyl(vinyl)silanediyl bis(oxy)bis(ethane-2,1-diyl) diacrylate) was obtained as a colorless liquid (M = 300.38 g/mol, yield: 58%).

FTIR (KBr, cm^{-1}): 3057 (–CH=CH_2), 2953 (–CH_2–), 2883 (–CH_2–), 1729 (C=O), 1639 (C=C, acrylic), 1598 (C=C, vinyl), 1299 (C–O); *^1H NMR* ($CDCl_3$, δ ppm): 6.40–6.46, 5.83–5.86 (CH_2=CH–COO–, d, 4H), 6.13–6.20 (CH_2=C*H*–COO–, m, 2H), 5.94–6.10 (CH_2=C*H*–Si, m, 3H), 4.25–4.31 (–COOC$H_2$$CH_2$–O–Si, t, 4H), 3.94–3.97 (–COOCH_2CH_2–O–Si, t, 4H), 0.23 (Si–CH_3, s, 3H); *Element analysis*: Calculated for $C_{13}H_{20}SiO_6$: C 51.98%, H 6.71%. Found: C 52.07%, H 6.64%.

2.2.2. Synthesis of M2

The monomer M2 (methyl(vinyl)silanediyl bis(oxy)bis(ethane-2,1-diyl) bis(2-methylacrylate)) was synthesized as a colorless liquid from 2-hydroxyethyl methylacrylate and vinylmethyldichlorosilane with a chemical route similar to that of M1 (M = 328.44 g/mol, yield: 54%).

FTIR (KBr, cm^{-1}): 3059 (–CH=CH_2), 2958 (–CH_2–), 2880 (–CH_2–), 1726 (C=O), 1639 (C=C, acrylic), 1598 (C=C, vinyl), 1299 (C–O); *^1H NMR* ($CDCl_3$, δ ppm): 6.13, 5.58 (CH_2=C(CH_3)–COO–, s, 4H), 5.96–6.10 (CH_2=C*H*–Si, m, 3H), 4.23–4.27 (–COOC$H_2$$CH_2$–O–Si, t, 4H), 3.94–3.97 (–COOCH_2CH_2–O–Si, t, 4H), 1.72 (CH_2=C(CH_3)–COO–, s, 6H), 0.23 (Si–CH_3, s, 3H); *Element analysis*: Calculated for $C_{15}H_{24}SiO_6$: C 54.86%, H 7.37%. Found: C 54.77%, H 7.34%.

2.2.3. Synthesis of A_2

1,1,3,3-Tetramethyl disiloxane (A_2) was synthesized as a colorless liquid (bp: 70 °C, 1.013 × 10^5 Pa) from dimethylchlorosilane as reported previously [21].

The Karstedt catalyst (a platinum–divinyltetramethyldisiloxane complex) was prepared according to Ref. [27].

2.2.4. Synthesis of P1 and its homologues

A_2 (1.34 g, 0.01 mol), M1 (3.00 g, 0.01 mol) and Karstedt catalyst (5 mg) were charged into a 50 mL flask equipped with magnetic stirrer. The reaction was conducted at 35 °C in air atmosphere, and monitored by FTIR. The reaction was finished until no Si–H absorption was detected from FTIR spectra (about 8 h). Thus, hyperbranched polymer P1 was obtained as a light yellow viscous liquid. P1-1.2, P1-1.1, P1-0.9, and P1-0.8 were prepared by changing the feeding molar ratios of A_2 and M1 from 1.0 to 1.2, 1.1, 0.9, and 0.8, respectively.

FTIR (KBr, cm^{-1}): 3108 (=CH, acrylic), 2957 (–CH_2–), 1724 (C=O), 1639 (C=C, acrylic), 1455 (–CH_2–), 1258 (Si–CH_3); *^1H NMR* ($CDCl_3$, δ ppm): 6.12, 5.56 (CH_2=CH–COO–), 5.83 (CH_2=C*H*–COO–), 4.22 (–COOC$H_2$$CH_2$–O–Si), 3.90 (–COOC$H_2CH_2$–O–Si), 1.25 (Si–$CH_2$–CH(C$H_3$)–), 1.01 (Si–CH(C$H_3$)–Si), 0.84 (Si–C$H_2$–CH($CH_3$)–), 0.45 (Si–$CH_2$–$CH_2$–Si), 0.02 (Si–C$H_3$).

2.2.5. Synthesis of P2

P2 was synthesized by using chemical routes similar to P1. The mole ratio of A_2 and M2 was 1.0. The reaction was also monitored on FTIR, and the reaction was completed about 6 h. The product was a light yellow viscous liquid and its molecular structure was characterized as follows:

FTIR (KBr, cm^{-1}): 3105 (=CH, acrylic), 2956 (–CH_2–), 1723 (C=O), 1638 (C=C, acrylic), 1454 (–CH_2–), 1257 (Si–CH_3); *^1H NMR* ($CDCl_3$, δ ppm): 6.09, 5.53 (CH_2=C(CH_3)–COO–), 4.20 (–COOC$H_2$$CH_2$–O–Si), 3.89 (–COOC$H_2CH_2$–O–Si), 2.50–2.55 (Si–$CH_2$–C*H*($CH_3$)–COO–, β addition product), 1.88–1.91 (CH_2=C(CH_3)–COO–), 1.12–1.17 (Si–C(CH_3)$_2$–COO–, α addition product; Si–CH_2–CH(CH_3)–COO–, β addition product), 0.99–1.01 (Si–CH(CH_3)–, α addition product), 0.64–0.72 (Si–CH_2–CH(CH_3)–COO–, β addition product), 0.45–0.51 (Si–CH_2–CH_2–, β addition product), 0.00–0.10 (Si–CH_3).

2.3. Instrumentation

FTIR spectroscopy (WQF-310, Rui Li Co. Beijing, China) was employed to characterize samples using thin KBr as the sample holder. The scanning range was set from 4000 to 400 cm^{-1}.

^{1}H NMR spectra were obtained on Avance 300 spectrometer, ^{13}C NMR and ^{29}Si NMR measurements were conducted on Avance 500 spectrometer (Bruker Biospin, Switzerland, frequency: 500 MHz) at 25 °C using $CDCl_3$ as solvent, and tetramethylsilane (TMS) as internal standard.

Elemental analysis was performed using a Vario (United States) EL III instrument.

SEC–MALLS measurement: The weight average molecular weight (M_w) was determined by size exclusion chromatography (SEC)/

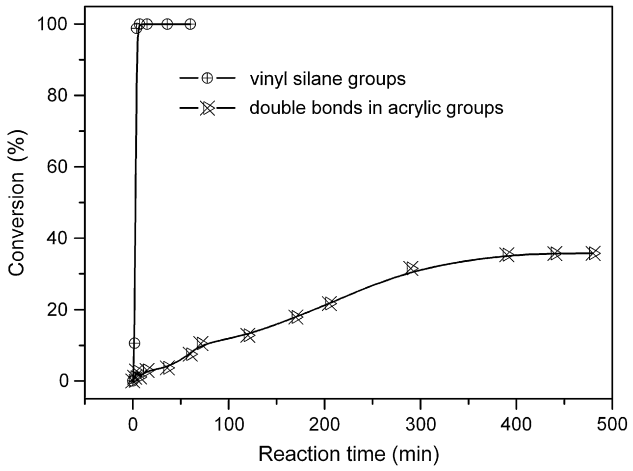

Fig. 1. Conversions of the reactive groups versus reaction time.

multi-angle laser light scattering (MALLS) instrument (Wyatt Technology Co., St. Barbara, USA). The chromatographic system consists of a Waters 515 pump, differential refractometer (Optilab rEX), and two columns, MZ 10^4 Å (300 × 6.8 mm) and MZ 10^3 Å (300 × 6.8 mm). The columns were kept at 25 °C in a thermostat. The HPLC grade tetrahydrofuran was used as solvent. The value of refractive index increment (d*n*/dc) (in THF, 25 °C) was measured on the refractive index instrument (Optilab rEX, Wyatt Technology Co., St. Barbara, USA). ASTRA software (Version 5.1.3.0) was used for data acquisition and analysis to calculate molecular weight of polymer.

DPC measurements were conducted on a differential scanning calorimeter (MDSC 2910, Waters-TA instrument, U.S.A.) equipped with a photo calorimeter accessory (Novacure 2100, EXFO Photonic Solutions Inc). The light source was a 100 W middle-pressure mercury lamp. UV light exposure intensities were set at 8.32 mW cm^{-2}, 19.41 mW cm^{-2}, 38.82 mW cm^{-2}, 61.01 mW cm^{-2} and 80.42 mW cm^{-2} (the actual light intensity exposed on specimens was approximately 10% of the set because the light source is at a distance of 20 mm from the sample [28]) over a wavelength range of 320–500 nm. Dosage of the samples was fixed at the range of 1.0–1.5 mg to eliminate the influence of coating thickness.

3. Results and discussion

3.1. Syntheses of monomers

M1 (methyl(vinyl)silanediylbis(oxy)bis(ethane-2,1-diyl) diacrylate) and M2 (methyl(vinyl)silanediylbis(oxy)bis(ethane-2,1-diyl)bis(2-methylacrylate)) were prepared via alcoholysis of vinylmethyldichlorosilane with 2-hydroxyethyl acrylate (or 2-hydroxyethyl methacrylate), respectively. The use of pyridine as HCl absorbent and 4-dimethylamino pyridine (DMAP) as catalyst can facilitate SiCl/OH condensation and improve the yield of objective products. The catalytic effects of DMAP and pyridine could be attributed to their strong nucleophilicity [11,19]. In the ^{1}H NMR spectrum, the chemical shift near 3.95 ppm can be assigned to the methylene proton bordered on silicon atom (Si–O–CH_2CH_2–OCO–), which demonstrates that the acrylate (or methacrylate) group was grafted on the silicon atom successfully. Furthermore, the molecular structure was also confirmed by means of FTIR and element analysis.

3.2. Synthesis of hyperbranched polymers

In the presence of Karstedt catalyst, the reaction of A_2 and CB_2 type monomers were carried out in bulk to avoid the influence of solvents on curing. The conversion of functional groups including vinyl (near 1600 cm^{-1} in FTIR) and acrylate or methacrylate (near 1640 cm^{-1}) groups can be calculated according to Eq. (1).

$$\text{Conversion}(\%) = \frac{A_0 - A_t}{A_0} \times 100\% \quad (1)$$

where A_0 represents the area of original absorption peak and A_t represents the peak area reacted for t min. For the reaction with equivalent A_2 and M2 at 35 °C, the conversion of vinyl and methacrylate groups versus reaction time is shown in Fig. 1, where it is clear that the synthesis process can be divided into two stages. At the first stage, the conversion of vinyl groups increased rapidly, and

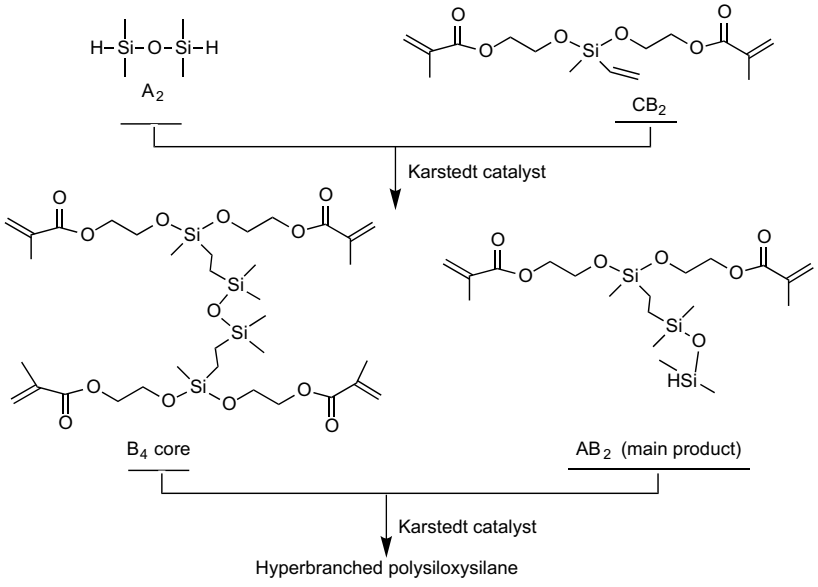

Scheme 1. The synthetic routes for UV curable hyperbranched polysiloxysilanes from A_2 and CB_2 monomers.

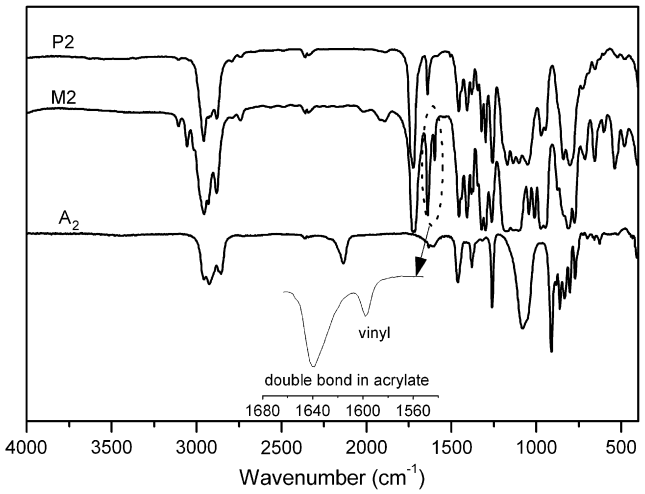

Fig. 2. FTIR spectra of A_2, M2, and P2.

reached 98% after 4 min. However, the conversion of methacrylate groups showed little change over the same period. This phenomenon indicated that hydrosilylation mainly occurred between vinyl and hydride silane groups during this stage, which results in the formation of two kinds of intermediates, including the dominant AB_2 (one molecule of A_2 react with one molecule of CB_2) and a small quantity of B_4 (one molecule of A_2 reacts with two molecules of CB_2) intermediates, as shown in Scheme 1. The reason can be attributed as follows: compared with methacrylate (or acrylate) groups, there is higher electron density in vinyl groups owing to the electron donating property of silicon atom, which results in higher reactivity of vinyl groups during hydrosilylation reaction.

During the second stage, the conversion of methacrylate groups increased and reached 35% after 400 min, and the conversion of methacrylate just reached 36% after 500 min, suggesting that intermediates formed in the first stage underwent further hydrosilylation to generate hyperbranched polysiloxysilane with methacrylate end groups. The reaction of A_2 and M1 was also monitored on FTIR, and similar phenomena were observed.

3.3. Characterization of hyperbranched polymers

The FTIR spectra of A_2, M2 and their resulting polymer P2 are shown in Fig. 2. From the FTIR spectrum of P2, the absorption peak

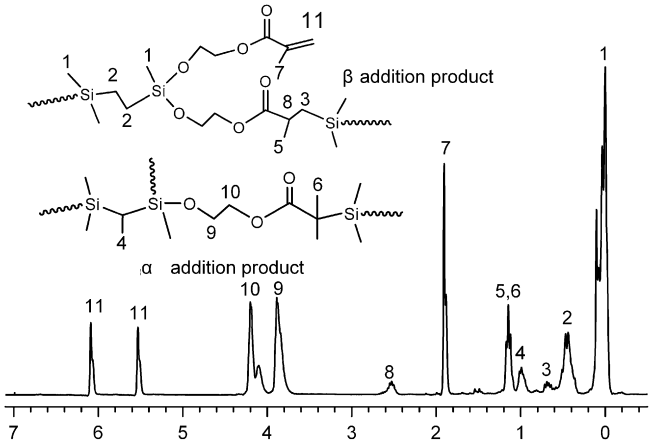

Fig. 3. ^{1}H NMR spectrum of P2.

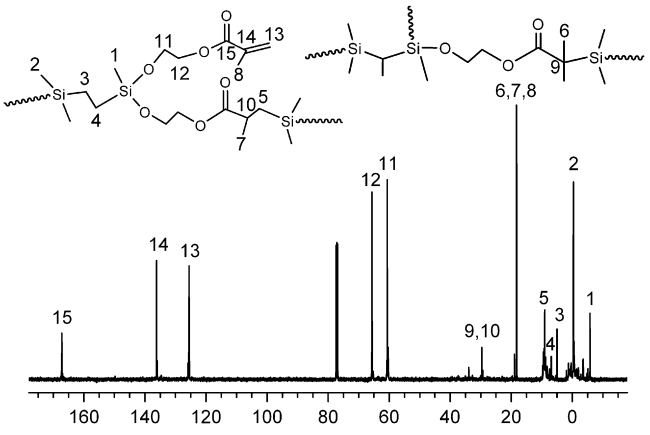

Fig. 4. ^{13}C NMR spectrum of P2.

of C=C bonds (1639 cm^{-1}) in methacrylate groups can still be observed, while absorptions of hydride silicon (2136 cm^{-1}) and vinyl groups (1598 cm^{-1}) have disappeared completely. Furthermore, in the ^{1}H NMR spectrum of P2 (Fig. 3), there are no chemical shifts for Si–H (4.73–4.75 ppm) and vinyl (5.96–6.05 ppm) groups, while the chemical shifts for methacrylate groups (6.09 ppm, 5.53 ppm) still exist. It is worth noting that certain new chemical shifts have appeared, which can be assigned to Si–CH_2–CH(CH_3)–COO– (2.50–2.55 ppm), Si–C(CH_3)$_2$–COO– and Si–CH_2–CH(CH_3)–COO– (1.12–1.17 ppm), Si–CH(CH_3)–Si– (0.99–1.01 ppm), Si–CH_2–CH(CH_3)–COO– (0.64–0.72 ppm) and Si–CH_2CH_2–Si– (0.45–0.51 ppm), respectively [29–31].

All the analyses above confirm that hydrosilylation reaction between A_2 and M2 monomers have been completed. Moreover, in the ^{1}H NMR spectrum of P2 (Fig. 3), relative integration of α and β addition signals shows that β addition product resulted from the hydrosilylation reaction of vinyl groups accounts to 71%, while the β addition ratio is about 55% in the hydrosilylation reaction of methacrylate groups. Similar results can also be obtained from analysis of ^{1}H NMR spectra of P1. The ^{13}C NMR spectrum of P2 shown in Fig. 4 further demonstrated that both α addition and β addition products existed in the polymer structure.

The degree of branching is an important parameter for hyperbranched polymers. We have characterized the branched structure utilizing ^{29}Si NMR spectrum (Fig. 5). There are only two main chemical shifts centered at 8.15 and −11.51 ppm. They can be assigned as the chemical shifts of silicon atoms bonded to one or

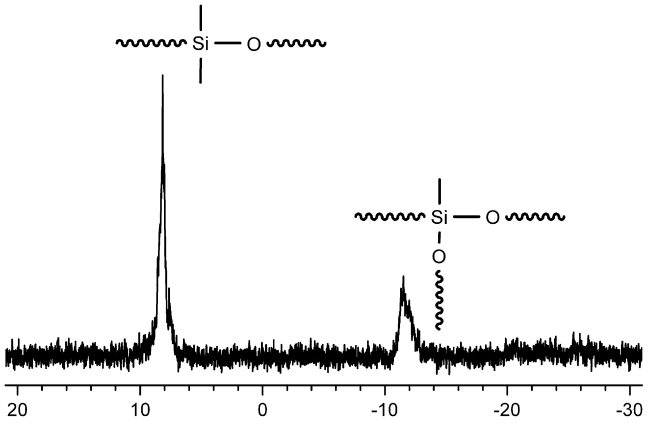

Fig. 5. ^{29}Si NMR spectrum of P2.

Table 1
Molecular parameters of polysiloxysilanes.

Sample	P1-0.8	P1-0.9	P1-1.2	P1-1.4	P1	P2
R^a	0.8	0.9	1.2	1.4	1.0	1.0
dn/dc	0.057	0.056	0.056	0.057	0.056	0.056
M_w	1960	2460	2840	1680	6990	5750
M_w/M_n	1.47	1.85	1.55	1.70	3.24	2.60
Intrinsic viscosity (mL/g)	2.8	2.2	2.7	2.6	4.1	2.9
Hydrodynamic radius (nm)	0.8	0.7	0.9	0.7	1.1	1.0
Mark–Houwink parameters α	0.50	0.39	0.41	0.43	0.39	0.46

[a] : The molar ratio of A_2 to CB_2 monomers.

two oxygen atoms [24,32], resulting from the original monomer A_2 and M1, respectively. Relative integration of the two chemical shifts is 1/0.47, in accord with the feeding ratio of monomers (1/0.5). For the chain unit that one silicon linked two oxygen atoms, there may be two (terminal unit), one (linear unit), or zero (dendritic unit) methacrylate group(s). However, their chemical shifts in ^{29}Si NMR spectrum are overlapped due to their similar structures, so it is difficult to obtain the degree of branching of the polymer direct from its ^{29}Si NMR.

Molecular weight and their distribution for linear polymers are usually determined on size exclusion chromatography (SEC) using linear polymer calibration standard. However, for hyperbranched polymers, their molecular sizes are smaller than the linear ones with the same molecular weights, as the effective sizes are related closely to the degree of branching [33]. It is therefore difficult to obtain exact molecular weight for hyperbranched polymers by general SEC procedures. Simultaneous measurements of light scattering intensity and concentration allow the direct determination of the weight average molecular weight for each eluted fraction without calibration by the standard materials [34]. In this investigation, SEC coupled with MALLS and refractive index detectors was used to determine molecular weights of hyperbranched polysiloxysilanes. The refractive index increments (dn/dc) of the polymers were determined using a refractive index (RI) detector, and the weight average molecular weights (M_w) were measured using a multi-angle laser light scattering detector. At the same time, other molecular structure parameters including intrinsic viscosity, hydrodynamic radius and Mark–Houwink parameters were obtained. As shown in Table 1, the polymer with higher molecular weight was obtained when equivalent monomers were used. Molecular weight of the polymers decreased rapidly when nonequivalent monomers were used. It should be noted that only oligomers can be obtained with increasing the disparity of the two monomers. This result may be attributed to A_2 or CB_2 monomer being exhausted during the initial stage of the reaction when nonequivalent monomers were used, which resulted in higher contents of oligomers.

Mark–Houwink (MH) equation exhibited relationship between intrinsic viscosity and molar mass of the polymer. It can be used to evaluate its molecular shape. The exponent α in MH equation depends on the molecular structure. Hard spheres give values of nearly 0; rigid rods give values ranging from 1 to 2; linear polymers exhibiting random coil structures give values ranging from 0.5 to 0.7, and hyperbranched polymers often give values below 0.5 except for those bearing end polar groups causing strong interactions with the solvent and resulting in an expansion of the molecular structure [10,35,36]. As shown in Table 1, the exponent α for all synthesized polysiloxysilanes is below 0.50, indicating molecular arrangements corresponding to hyperbranched structures. The analyses above clearly show that hyperbranched polysiloxysilanes have been obtained successfully.

3.4. UV curing behavior

The synthesized hyperbranched polysiloxysilanes with a general photoinitiator IHT-PI 185 can be cured under UV irradiation either in nitrogen or under the open atmosphere. The UV curing process was monitored by differential scanning photocalorimeter (DPC). The heat flow was assumed to be proportional to the polymerization rate during UV curing. Therefore the rate of polymerization (R_p) can be defined as follows:

$$R_p = \frac{d\alpha}{dt} = \frac{1}{\Delta H_{th}} \frac{dH}{dt} \quad (2)$$

where dα/dt is polymerization rate (R_p), dH/dt is measured heat flow, and the theoretical enthalpy ΔH_{th} is replaced by the maximum polymerization enthalpy for the same formulation in this investigation. The degree of conversion is calculated from the integrated form of Eq. (2)

$$\alpha_t = \frac{\Delta H_t}{\Delta H_{th}} \times 100\%. \quad (3)$$

where α_t is the degree of conversion at time t, and ΔH_t is the cumulative heat of reaction up to time t.

3.4.1. Influence of photoinitiator concentration

The influence of photoinitiator concentration on the curing behavior at 20 °C was studied using P1 as the model polymer. The light intensity was set at 38.82 mW cm^{-2}, and the photoinitiator concentration varied from 1.06% to 7.35% (w/w). Polymerization

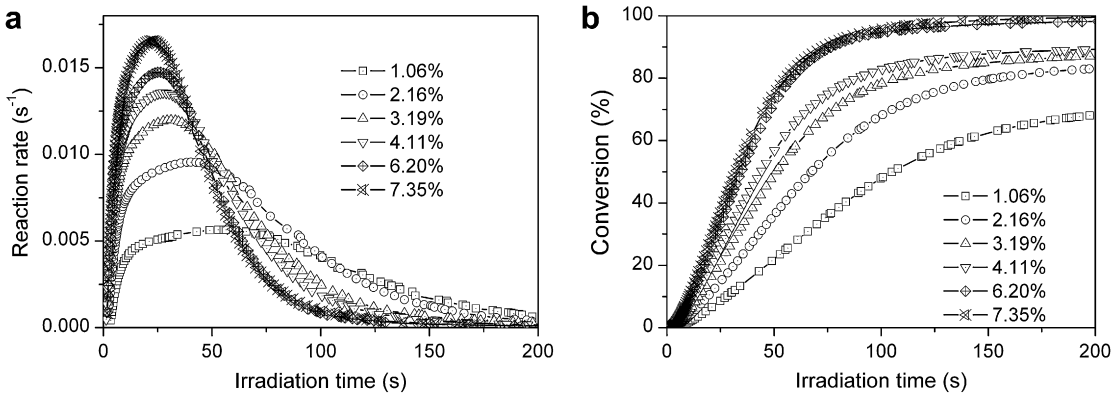

Fig. 6. Influence of the content of photoinitiator on polymerization rate (a) and conversion (b) of P1, light intensity: 38.82 mW cm^{-2}, 20 °C.

Table 2
UV curing parameters of P1 systems using different content of photoinitiator.

Initiator concentration (%)	t_i (s)	t_p (s)	$R_p \times 100$ (s^{-1})	$\alpha_p \times 100$	$\alpha_f \times 100$
1.06	8.20	55.41	0.56	24.99	70.47
2.16	5.93	40.24	0.96	27.65	84.31
3.19	4.85	31.15	1.20	28.19	88.25
4.11	4.23	27.46	1.36	28.55	89.80
6.20	4.07	24.97	1.47	33.05	98.69
7.35	3.93	22.92	1.65	32.54	100.00

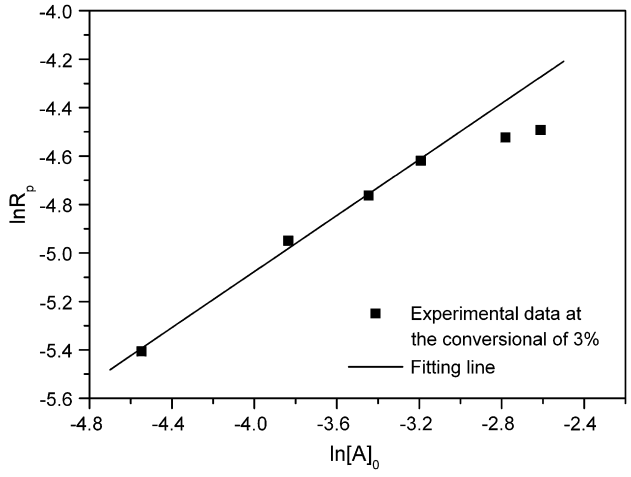

Fig. 7. The relationship curve of ln R_p and ln $[A]_0$.

rate and conversion in nitrogen atmosphere versus irradiation time are presented in Fig. 6. The detailed polymerization parameters, such as t_i (induction time, the time to attain 1% of conversion), a_f (the final conversion), and t_p, R_p, and α_p (the time, rate and conversion at the maximum polymerization rate, respectively) are listed in Table 2. It can be found that the maximum polymerization rate R_p and the final conversion a_f are improved with the increased photoinitiator concentration. Moreover, t_p decreased with increased photoinitiator concentration. It was attributed to the very low initiator concentration yielding few radicals under light irradiation, leading to a long period of time to attain the gel stage producing the maximum rate in the polymerization.

During the initial stage of the photo polymerization ($a = 3\%$), it could be assumed that the polymerization was controlled by the initiating rate, and the rate of photo polymerization can be expressed as Eq. (4) [37].

$$R_p = -\frac{d[M]}{dt} = \frac{k_p}{k_t^{0.5}}[M](\phi\varepsilon[A_0])^{0.5}(I_0)^{0.5} \quad (4)$$

where k_p and k_t are the propagation and termination rate constants, $[M]$ is the initiation efficiency, φ is the quantum yield, ε is the absorption coefficient, I_0 is the initial light intensity, and $[A]$ is the photoinitiator concentration.

Fig. 7 presents the double logarithmic plots of R_p and $[A]_0$ at the conversion of 3%. The polymerization rate R_p increases with increased initiator concentration $[A]_0$. There is a clear linear relationship between ln R_p and ln $[A]_0$ when the initiator concentration below 4.11%. The slope of the linear fit is 0.51, showing a consistency with the trend predicted by Eq. (4). However, when the initiator concentration is higher than 4.11%, the experiment data starts to deviate from the linearity. The deviation might be attributed to the decrease of quantum yield φ when the initiator concentration increased. It is expected that the initiating rate is proportional to the primary radical $[A^*]$, and the coupling rate of two radicals is proportional to $[A^*]^2$. Quantum yield φ is determined by the result of the competition, the more $[A^*]$, and the less φ. Considering the negative effect of excess initiator on the physical and chemical properties of the cured polymer, the concentration of photoinitiator will be fixed at 4.11% in the following research.

3.4.2. Influence of light intensity

In the presence of 4.11% photoinitiator, isothermal DPC measurements were carried out at 20 °C, and the light intensity was ranged from 8.32 to 80.42 mW cm^{-2}. Fig. 8 shows the dependence of polymerization rate and conversion on irradiation time under nitrogen. It can be seen that the polymerization rate increased with light intensity. However, the effect on final conversion exhibited a different regulation. It was increased with the increase of light intensity and then was decreased with the further decrease of light intensity after a maximum. The results may be attributed to the combined influence of free volume and glass formation [38–40]. Photopolymerization rates were relatively high, and reactive cross-linking systems could not be in volume equilibrium because volume shrinkage rates were much slower than chemical reaction rates. The process resulted in temporary excesses of free volumes and the increase in mobility of residual reactive groups and active centers. Thus, the higher light intensity led to the higher polymerization rate. The onset of vitrification of the curing system was brought forward when the reaction rate increased, as a consequence of increasing light intensity. At this time, the reaction became diffusion controlled at a comparatively low conversion. Therefore, the final conversion decreased when the light intensity exceeded a certain value.

The influence of light intensity in air atmosphere was also studied, and similar result was found as presented in Fig. 9. The

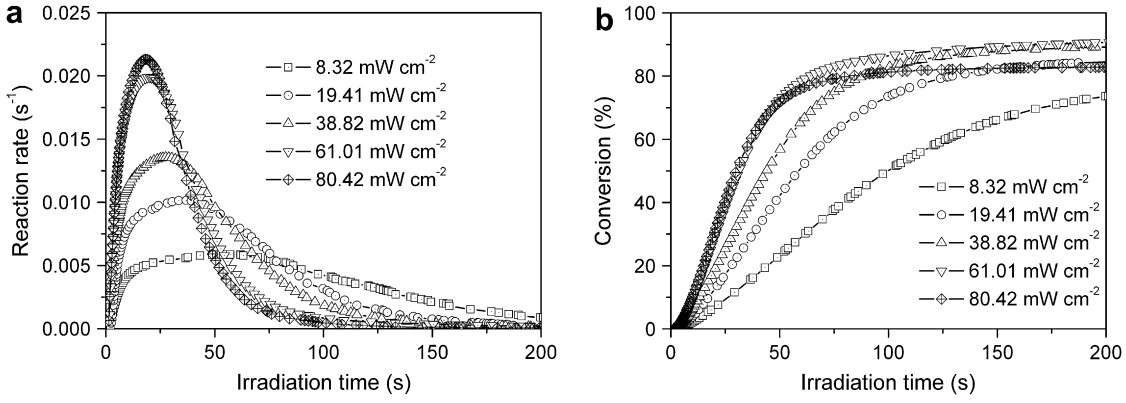

Fig. 8. Influence of light intensity on polymerization rate (a) and conversion (b) of P1, at 20 °C, in nitrogen atmosphere.

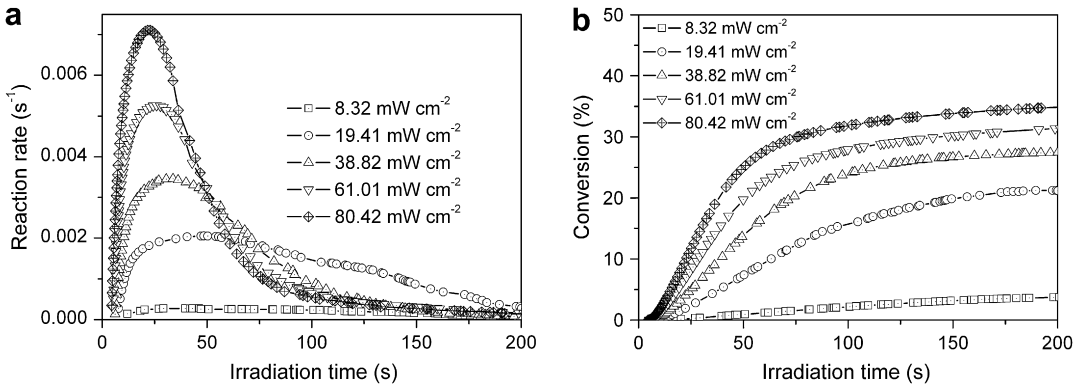

Fig. 9. Influence of light intensity on polymerization rate (a) and conversion (b) of P1, at 20 °C, in air atmosphere.

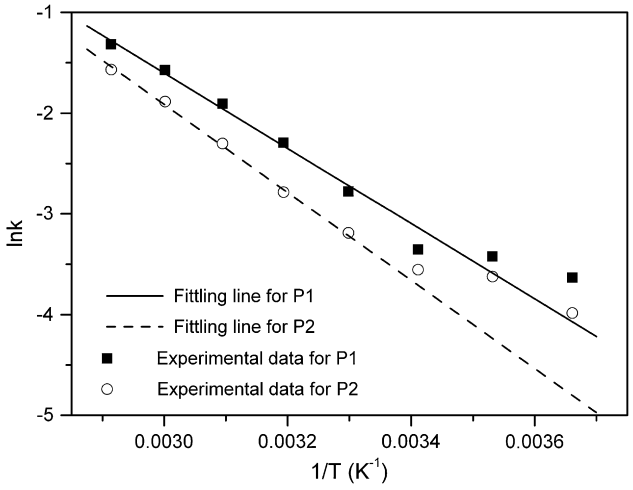

Fig. 10. The relationship curves between ln k and $1/T$.

inhibition effect of oxygen was observed when the reaction was performed in air. R_p and a_f in air were lower than those under nitrogen protection with the same light intensity. The final conversion in air was only 3.7% under the light intensity of 8.32 mW cm^{-2}, and R_p and a increased rapidly with the increase of light intensity. This result indicates that the inhibition effect of oxygen can be reduced by increasing the light intensity.

3.5. Investigation of UV curing kinetics

Figs. 6–8 show typical auto-accelerative reaction characteristics and glass effect phenomena. The auto-accelerative gel effect occurs under irradiation for a few seconds, implying the restricted segmental movement of radicals and diffusion-controlled termination. During this stage, k_t in Eq. (4) decreases sharply, resulting in a dramatic improvement in R_p. As the reaction continues, the viscosity of the system increases and the propagation reaction becomes diffusion controlled model. At this stage, k_p in Eq. (4) also decreases, resulting in the so called glass effect, i.e. an obvious decrease of R_p [41]. The process is often described as the model developed by Kamal [42,43].

$$R_p = \frac{d\alpha}{dt} = k\alpha^m(\alpha_f - a)^n \tag{5}$$

where n is the order of reaction and m is the auto-accelerative exponent, k is the reaction rate constant, α_f is the final conversion, described as the ratio of the total exothermal heat of each reaction to the maximum exothermal heat with the same composition. Applying Eq. (5) to this system, kinetic parameters, such as k, m, and n, can be obtained using a least square regression method to fit our experimental data to the model (using the software of MatLab 7.1). The total orders of the UV curing reaction for two polymers are 1.5 and 1.67 deduced from the average values of $m + n$. Moreover, according to Arrehenius equation, the reaction rate constant can be expressed by Eq. (6).

$$k = A\exp\left(-\frac{E_a}{RT}\right) \tag{6}$$

where A is the pre-exponential factor, E_a is the activation energy, R is the gas constant, and T is the absolute temperature. From the logarithmic form of Eq. (6), E_a can be obtained from the slope of ln k versus $1/T$ plot:

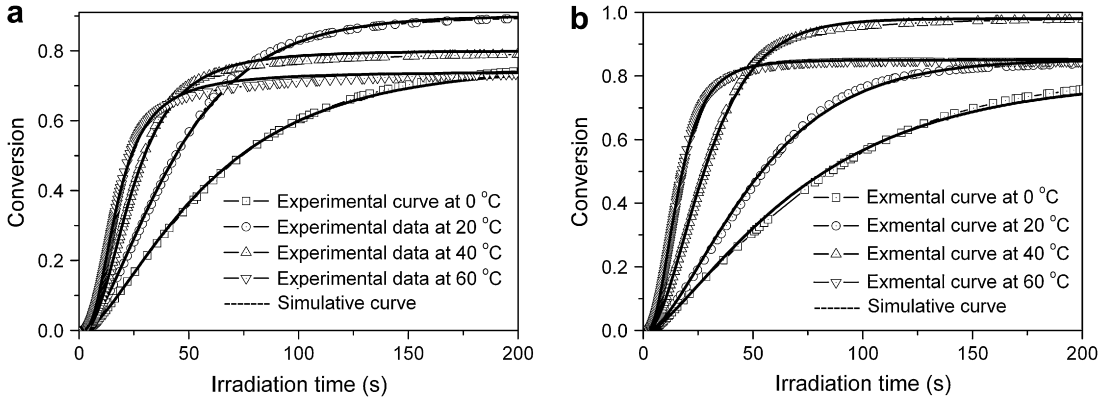

Fig. 11. Comparisons between experiments and the model for P1 (a), P2 (b).

$$\ln k = \ln A - \frac{E_a}{RT} \quad (7)$$

The ln k versus $1/T$ plots for different polymers are shown in Fig. 10. It can be seen that the experimental data are linear for all the polymers when the values of $1/T$ are below 0.0034 K^{-1} (the reaction was above 20 °C). However, the experimental data start to deviate from the linear relation below 20 °C. This deviation may be associated with the glass transition of the cured polymers. Our previous work revealed that the T_g values of similar cured polymers were about 20 °C, which must have an impact on the activation energy of the curing reactions [38]. Activation energy E_a was obtained from the fittings above 20 °C, which is 31.05 and 36.32 kJ/mol for polymer P1 and P2, respectively. Fig. 11 compares the experimental data of conversion and those obtained from the graph plotted using Eq. (5). Excellent agreements observed in Fig. 11 indicate that the model developed by Kamal is well suited to studying the UV curing kinetics of the hyperbranched polysiloxysilanes.

4. Conclusions

The polysiloxysilanes prepared using $A_2 + CB_2$ approach could be cured rapidly under UV light irradiation. The reaction rates increased with the increase of concentration of photoinitiator and light intensity. The inhibition effect of oxygen was nonnegligible when the reaction performed in air, and it was decreased with the increase of light intensity. Furthermore, the study of UV curing kinetics indicate that the total orders of the UV curing reaction for P1 and P2 are 1.50 and 1.67, and the activation energy is 31.05 and 36.32 kJ/mol, respectively.

Acknowledgements

The authors gratefully acknowledge the supports of *the Specialized Research fund for the Doctoral Program of Higher Education* (No. 200804251523) and *National Natural Science Foundation of China* (No. 20874080).

References

[1] Gao C, Yan D. Prog Polym Sci 2004;29:183–275.
[2] Kim YH. J Polym Sci Part A Polym Chem 1998;36:1685–98.
[3] Vöit B. J Polym Sci Part A Polym Chem 2000;38:2505–25.
[4] Ratna D, Becker O, Krishnamurthy R, Simon GP, Varley RJ. Polymer 2003;43:7449–57.
[5] Wang SJ, Fan XD, Liu X, Kong J, Liu YY, Wang X. Polym Int 2007;56:764–72.
[6] Hans R, Kricheldorf HR, Bornhorst K. J Polym Sci Part A Polym Chem 2007;45:5597–605.
[7] Esumi K. Top Curr Chem 2003;227:31–52.
[8] Frey H, Lach C, Lorenz K. Adv Mater 1998;10:279–93.
[9] Bischoff R, Cray SE. Prog Polym Sci 1999;24:185–219.
[10] Vöit B. J Polym Sci Part A Polym Chem 2005;43:2679–99.
[11] Miravet JF, Fréchet JMJ. Macromolecules 1998;31:3461–8.
[12] Wideman T, Fazen PJ, Su K, Remsen EE, Zank G, Sneddon LG. Appl Organometal Chem 1998;12:681–93.
[13] Bill J, Aldinger F. Adv Mater 1995;7:775–87.
[14] Lang H, Lühmann B. Adv Mater 2001;13:1523–40.
[15] Kroke E, Li YL, Konetschny C, Lecomte E, Fasel C, Riedel R. Mater Sci Eng R 2000;26:97–199.
[16] Andrzejewska E, Podgorska-Golubska M, Stepniak I, Andrzejewski M. Polymer 2009;50:2040–7.
[17] Rufs AM, Valdebenito A, Rezende MC, Bertolotti S, Previtali C, Encinas MV. Polymer 2008;49:3671–6.
[18] Owusu-Adom K, Guymon CA. Polymer 2008;49:2636–43.
[19] Si QF, Wang X, Fan XD, Wang SJ. J Polym Sci Part A Polym Chem 2005;43:1883–94.
[20] Wang SJ, Fan XD, Kong J, Wang X, Zhang GB. Acta Polym Sin 2006;8:1024–8.
[21] Wang SJ, Fan XD, Kong J, Wang X, Liu YY, Zhang GB. J Polym Sci Part A Polym Chem 2008;46:2708–20.
[22] Wang SJ, Fan XD, Kong J, Liu YY. J App Polym Sci 2008;107:3812–22.
[23] Cranat P, Pudas M, Hormi O, Hagberg J, Leppavuori S. Carbohydr Polym 2004;57:225–8.
[24] Kong J, Fan XD, Zhang GB, Xie X, Si QF, Wang SJ. Polymer 2006;47:1519–25.
[25] Mirschel G, Heymann K, Scherzer T, Buchmeiser MR. Polymer 2009;50:1895–900.
[26] Cramer NB, O'Brien CP, Bowman CN. Polymer 2008;49:4756–61.
[27] Karstedt BD, USP 3 775 452, 1973-11-27.
[28] User handbook of photo calorimeter accessory. America: Waters-TA Co.; 2003. p. 21–2.
[29] Wang SJ, Fan XD, Si QF, Kong J, Zhang GB. Acta Polym Sin 2006;5:707–11.
[30] Vasilenko NG, Rebrov EA. Macromol Chem Phys 1998;199:889–95.
[31] Buschbeck R, Lang H. Inorg Chem Commun 2004;7:1213–6.
[32] Hook RJ. J Non-Cryst Solids 1996;195:1–15.
[33] Grcev S, Schoenmakers P, Ledema P. Polymer 2004;45:39–48.
[34] Kong J, Fan XD, Si QF, Zhang GB, Wang SJ, Wang X. J Polym Sci Part A Polym Chem 2006;44:3930–41.
[35] Jaumann M, Rebrov EA, Kazakova VV, Muzafarov AM, Goedel WA, Möller M. Macromol Chem Phys 2003;204:1014–26.
[36] Simon PFW, Müller AHE, Pakula T. Macromolecules 2001;34:1677–84.
[37] Jiang X, Xu H, Yin J. Polymer 2004;45:133–40.
[38] Lecamp L, Youssef B, Bunel C. Polymer 1997;38:6089–96.
[39] Maffezzoli A, Terzi R. Thermochim Acta 1998;321:111–21.
[40] Atai M, Watts DC. Dent Mater 2006;22:785–91.
[41] Kamal MR, Sourour S. Polym Eng Sci 1973;13:59–64.
[42] Kamal MR. Polym Eng Sci 1974;14:231–9.
[43] Xiao Y, Son Y. J Polym Sci Part A Polym Chem 2001;39:3383–91.